TERM CrossMark

ORIGINAL ARTICLE

Cellular Response of Human Bone Marrow Derived Mesenchymal Stem Cells to Titanium Surfaces Implanted with Calcium and Magnesium Ions

Sun Won[1] · Yoon-Hyuk Huh[1] · Lee-Ra Cho[1] · Hee-Su Lee[2] · Eung-Sun Byon[3] · Chan-Jin Park[1]

Abstract Surface characteristics and cellular response to titanium surfaces that had been implanted with calcium and magnesium ions using plasma immersion ion implantation and deposition (PIIID) were evaluated. Three different titanium surfaces were analyzed: a resorbable blast media (RBM) surface (blasted with hydroxyapatite grit), a calcium ion-implanted surface, and a magnesium ion-implanted surface. The surface characteristics were investigated by scanning electron microscopy (SEM), surface roughness testing, X-ray diffraction (XRD), and Auger electron spectroscopy (AES). Human bone marrow derived mesenchymal stem cells were cultured on the 3 different surfaces. Initial cell attachment was evaluated by SEM, and cell proliferation was determined using MTT assay. Real-time polymerase chain reaction (PCR) was used to quantify osteoblastic gene expression (i.e., genes encoding RUNX2, type I collagen, alkaline phosphatase, and osteocalcin). Surface analysis did not reveal any changes in surface topography after ion implantation. AES revealed that magnesium ions were present in deeper layers than calcium ions. The calcium ion- and magnesium ion-implanted surfaces showed greater initial cell attachment. Investigation of cell proliferation revealed no significant difference among the groups. After 6 days of cultivation, the expression of RUNX2 was higher in the magnesium ion-implanted surface and the expression of osteocalcin was lower in the calcium ion-implanted surface. In conclusion, ion implantation using the PIIID technique changed the surface chemistry without changing the topography. Calcium ion- and magnesium ion-implanted surfaces showed greater initial cellular attachment.

Keywords Human bone marrow derived mesenchymal stem cells · Plasma immersion ion implantation and deposition (PIIID) · Calcium ion · Magnesium ion · Osteogenesis

✉ Chan-Jin Park
doctorcj@gwnu.ac.kr

1 Department of Prosthodontics and Research Institute of Oral Science, College of Dentistry, Gangneung-Wonju National University, Jukheongil 7, Gangneung, Gangwon-do 26403, Republic of Korea

2 Department of Anatomy and Research Institute of Oral Science, College of Dentistry, Gangneung-Wonju National University, Gangwon-do 26403, Republic of Korea

3 Materials Processing Division, Korea Institute of Materials Science, 797 Changwondaero, Seongsan-gu, Changwon, Gyeongnam 51508, Republic of Korea

1 Introduction

Implant surface characteristics such as topography, roughness, physical properties, and chemical composition can be modified [1]. Surface innovation has been focused on surface topographic changes for improved osseointegration. Various techniques, such as spraying, sintering, beading, grit blasting, etching, and hybrid techniques, have been suggested for modifying the surface topography or roughness of dental implants [2]. Surface chemistry plays an important role in the regulation of the interaction between the implant surface and cells. Several chemical modification methods, such as sol-gel processing [3], heat treatment [4], anodic oxidation [5], and ion implantation

[6, 7], have been proposed to enhance biochemical interlocking and cellular response.

Ion implantation is a material engineering process by which ions are accelerated in an electrical field and impacted onto the surface of a substrate to change the surface chemistry [8]. Plasma source ion implantation (PSII) has been developed to overcome the line-of-sight limitations of traditional beam line ion implantation [9, 10]. Plasma immersion ion implantation and deposition (PIIID) is another term for emphasizing the cyclic process of repeating cathodic arc deposition and PSII using condensable metal plasmas. Several studies have reported the implantation of titanium surfaces by bioactive ions, such as those of fluorine (F) [11], sulfur (S) [12], phosphorus (P) [12], calcium (Ca) [6, 7, 13–15], and magnesium (Mg) [16–20].

The Ca ions in the $CaTiO_3$ layer may play a role in apatite formation because a greater number of phosphate ions can be absorbed, resulting in the acceleration of calcium phosphate formation [21]. Calcium phosphate formation has also been reported to upregulate the expression of genes related to bone formation and remodeling [6]. Mg ions are known to be involved in the binding interaction of the integrin superfamily of cell surface receptors and ligand proteins, including fibronectin, vitronectin, fibrinogen, and some cell-to-cell adhesion receptors [22–25]. Therefore, Ca ion- and Mg ion-implanted titanium implants have demonstrated superior osseointegration and cellular response in several *in vitro* and *in vivo* studies [16–18].

Cell culture models allow controlled experimental conditions [26]. With primary cells or osteoblast-like cell lines, the interaction between the bone cells and the implant surface modifications can be evaluated. Human bone marrow derived mesenchymal stem cells (hBM-MSCs) are multi-lineage potential cells that are able to self-renew and differentiate into every type of cell, such as osteoblasts, chondrocytes, endothelial cells, adipogenic cells, and neuronal-like cells [27]. hBM-MSCs play an essential role in osteoinduction, osteogenesis, and bone reparative mechanisms, including osseointegration of implants [28]. Osteoblasts related to osseointegration mainly originate from progenitor cells in the periosteum, and multipotent mesenchymal stem cells originate in the bone marrow [29]. With hBM-MSCs, responses similar to those occurring *in vivo* can be evaluated more easily in the early stages of immature mesenchymal stem cell attachment and proliferation.

In this study, the cellular responses of hBM-MSCs to titanium that had been chemically modified by Ca ion or Mg ion implantation were examined to evaluate the quality of titanium implant osseointegration. The aims of this study were to assess the topographical and chemical changes resulting from Ca ion and Mg ion implantation. The cellular response of hBM-MSCs to Ca ion- and Mg ion-implanted titanium surfaces was compared with resorbable blast media (RBM)-treated titanium surfaces by observing cell attachment, proliferation, and gene expression in the osteoblastic phenotypes.

2 Materials and methods

2.1 Preparation of specimens

Three different titanium surfaces were analyzed: an RBM surface (control), a Ca ion-implanted surface, and an Mg ion-implanted surface. Cylindrical disks (10 mm diameter and 1 mm thick), made from commercially pure titanium (ASTM grade 4), were prepared. All disks were ultrasonically cleaned in acetone and alcohol for 15 min and then dried. RBM surface treatment was conducted by grit blasting with hydroxyapatite (HA). For the test groups, Ca and Mg ions were implanted onto the RBM-treated surfaces using the PIIID technique. Highly ionized Ca and Mg plasmas were generated from a filtered vacuum arc source and then accelerated within the electric field between a sheath and the substrates. The energy of the implantation field was 10 keV, and the retained dose was 5.0×10^{15} ions/cm^2. After ion implantation, all disks were enveloped and sterilized with γ-radiation from a ^{60}Co source, with a dose rate of 30 kGy. All specimens were provided by the DIO Implant Corporation (Busan, Korea).

2.2 Surface analysis

The surface topographical change was investigated by surface roughness evaluation and scanning electron microscopy (SEM) (VEGA; TESCAN, Seoul, Korea). Surface roughness was measured using a surface roughness tester (TR200; CV Instruments Europe BV, London, UK). Three disks representing the groups were investigated. Measurements were performed twice on each disk to calculate the average surface roughness (Ra) values. The surface morphologies of the specimens were observed using SEM (VEGA) at 500× and 2,000× magnification. The crystalline structure and chemical composition of the TiO_2 layer were evaluated using a thin-film X-ray diffractometer (XRD) (X'Pert^3 Powder; PANalytical BV, Almelo, Netherlands). The step size of the measured scan was 0.02° between 15° and 80°. The spectra were recorded using Cu K-alpha radiation. Auger electron spectroscopy (AES) (PHI650; Physical Electronics, Chanhassen, USA) analysis was used to determine the underlying elemental compositions from the outermost surface to the inner layer. A primary electron beam of 3 keV and 2.6 μA with a diameter of 40 μm was used for electron excitation. During

depth profiling, the specimens were sputtered using 2 symmetrically inclined 1 keV Ar ion beams at an ion incidence angle of 47° to the surface normal. The atomic concentrations were calculated using the relative sensitivity factors given by the instrument producer.

2.3 Cell culture

hBM-MSCs were obtained from commercial sources (ATCC, Manassas, USA). Cells were cultured in American Type Culture Collection (ATCC) basal medium supplemented with 7% fetal bovine serum (FBS), rh IGF-1 (15 ng/mL), Rh FGF-b (125 pg/mL), L-alanyl-L-glutamine (2.4 mM), penicillin (10 units/mL), streptomycin (10 µg/mL), and amphotericin B (25 µg/mL) solutions. Cells were maintained at 37°C in a 5% CO_2 humidified atmosphere. The culture medium was changed every 3 days.

2.4 Cell attachment morphology

For assessment of initial cell attachment configuration, initial hBM-MSC attachment morphology was evaluated by SEM (VEGA). The cells were seeded at 1×10^5/well. Cells were cultured on the 3 different disks in 24-well plate for 4, 24, and 48 h. The cells were fixed with 2.5% glutaraldehyde (50 µL), dehydrated by a series of ethanol washes (70, 90, and 100%), and refixed with hexamethyldisilazane. The specimens were then sputter-coated with gold and investigated using SEM (VEGA) at an accelerating voltage of 10 kV.

2.5 Cell proliferation

For assessment of cell proliferation, hBM-MSCs were assessed using a 3-(4,5-dimethylthiazol-2-yl)-2,5-diphenyltetrazolium bromide (MTT) assay. The cells were seeded at 1×10^5/well. At 24 and 48 h after plating on the 24-well plate, non-adherent cells were washed off with phosphate buffer solution (PBS). The MTT solution (50 µL), prewarmed to 37°C, was added to each well and then incubated for 4 h. After incubation, the formazan dyes were dissolved using 0.04 N HCl isopropanol (400 µL). Each solution was then transferred to a 96-well plate and its optical density at 570 nm was measured using a microplate analyzer (Model EL312e Bio-Kinetics Microplate Reader, BioTek Instruments, Winooski, VT, USA).

2.6 Osteogenic differentiation

To examine osteogenic differentiation, cells seeded onto the 3 different disks were analyzed by real-time polymerase chain reaction (PCR) after 6 days of culture. Total RNA from the specimens was extracted using an RNeasy Mini Kit (QIAGEN GmbH, Hilden, Germany) according to the manufacturer's instructions. DNAse treatment was carried out to eliminate any contamination from genomic DNA. The primers for the genes that encode RUNX2, type 1 collagen, alkaline phosphatase (ALP), osteocalcin (OC), and glyceraldehyde-3-phosphate dehydrogenase (GAPDH) are presented in Table 1, and were used for quantitative real-time PCR. Real-time PCR was performed in duplicate using the Mastercycler ep realplex (Eppendorf, Hamburg, Germany) in a volume of 20 µL. The PCR conditions were as follows: 95°C for 10 min, followed by 45 cycles of 95°C for 20 s, 60°C for 20 s, and 72°C for 20 s. The fluorescence was determined at the end of the 72°C step. Melting curves were created from the data recorded during a stepwise temperature increase (1°C/5 seconds) from 60 to 95°C. Target gene expression was normalized to GAPDH (defined as the house-keeping gene) expression. Normalized relative quantities were calculated using the delta Ct method and 90% PCR efficiency.

2.7 Statistical analysis

The data were analyzed using IBM SPSS version 21.0 (SPSS Inc., Chicago, USA). Surface roughness (Ra) values were statistically analyzed using a non-parametric Kruskal–Wallis test. The results of the MTT assay were subjected to one-way analysis of variance (ANOVA) followed by Scheffé's multiple comparison for post hoc comparisons. Statistical significance was established at a 95% confidence level.

3 Results

3.1 Surface analysis

To investigate surface topographical changes, surface roughness and SEM images were evaluated. The control (RBM surface) group and test (Ca and Mg ion-implanted

Table 1 Primers used in real-time polymerase chain reaction

Genes	Primers (F; forward, R; reverse)
RUNX2	F: CAGACCAGCAGCACTCCATA
	R: CAGCGTCAACACCATCATTC
Type I collagen	F: AAGAGGAAGGCCAAGTCGAG
	R: TAAGACAGCTGGGGAGCAAA
ALP	F: CCACGTCTTCACATTTGGTG
	R: AGACTGCGCCTGGTAGTTGT
OC	F: TGAGAGCCCTCACACTCCTC
	R: CGCCTGGGTCTCTTCACTAC
GAPDH	F: TGAAGGTCGGAGTCAACGGAT
	R: TTCTCAGCCTTGACGGTGCCA

surface) groups showed similar Ra values ranging from 0.91 to 0.92 μm ($P > .05$). The SEM images revealed that all 3 titanium surfaces were irregular and had rough morphology, as generally observed in RBM grit-blasted titanium surfaces (Fig. 1). The delamination of deposited films or the clustering of deposited particles was not observed at the ion-implanted surfaces. There were no obvious changes in surface topography after ion implantation.

XRD analysis showed no changes in the crystalline structure and no newly formed compounds following Ca ion and Mg ion implantation by PIIID (Fig. 2).

The AES depth profile showed a graded surface structure of the Ca ion- and Mg ion-implanted titanium oxide layer (Fig. 3). The ion concentration of Ca, Mg, and titanium varied gradually from the outermost surface to the bulk without forming a distinct interface. On the outermost surface, the atomic concentrations of Ca and Mg ions were 15% and 12%, respectively. Mg ions were present in deeper layers than Ca ions. The presence of oxygen in the implanted layer indicated that calcium and magnesium oxides were formed during ion implantation. More oxygen was present in the Ca ion- than in the Mg ion-implanted surface. Carbon ions, regarded as remnants of the manufacturing procedure, were observed to a greater degree and at a deeper level in the Ca ion-implanted surface layer.

3.2 Cell attachment morphology

The SEM images used for the assessment of initial cell attachment morphology are shown in Fig. 4. After 4 h of cultivation, a greater number of cells were attached to the Ca ion-implanted surface. Cells on the Mg ion-implanted surface presented a wide extracellular membrane bridge and a flattened morphology compared with the RBM surface. After 24 h, there were no distinguishable differences between the RBM and Mg ion-implanted surfaces. However, cells attached to the Ca ion-implanted surface presented more extended filopodia compared with those on the RBM and Mg ion-implanted surfaces. After 48 h, there were more cells on all surfaces and there was no obvious difference among the groups.

3.3 Cell proliferation

At both 24 and 48 h of cultivation, there were no differences among the three different surfaces. However, cell proliferation on all surfaces was significantly increased after 48 h compared with 24 h of cultivation (Fig. 5).

3.4 Osteogenic differentiation

The results of the quantitative real-time PCR analysis of the mRNA levels of RUNX2, type I collagen, ALP, and
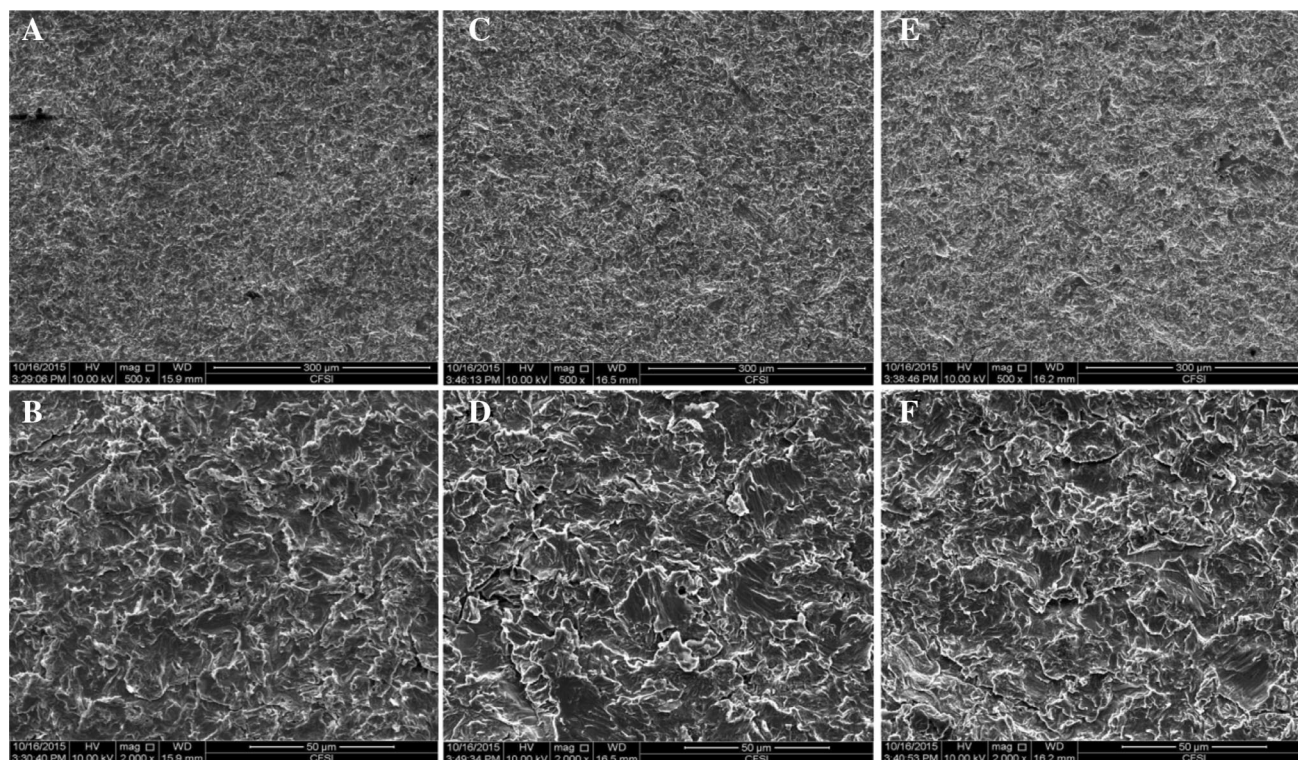

Fig. 1 Scanning electron microscopy (SEM) images. The resorbable blast media (RBM) surface (**A**, **B**), the Ca ion-implanted surface (**C**, **D**), and the Mg ion-implanted surface (**E**, **F**) at magnifications of ×500 (**A**, **C**, **E**) and ×2,000 (**B**, **D**, **F**)
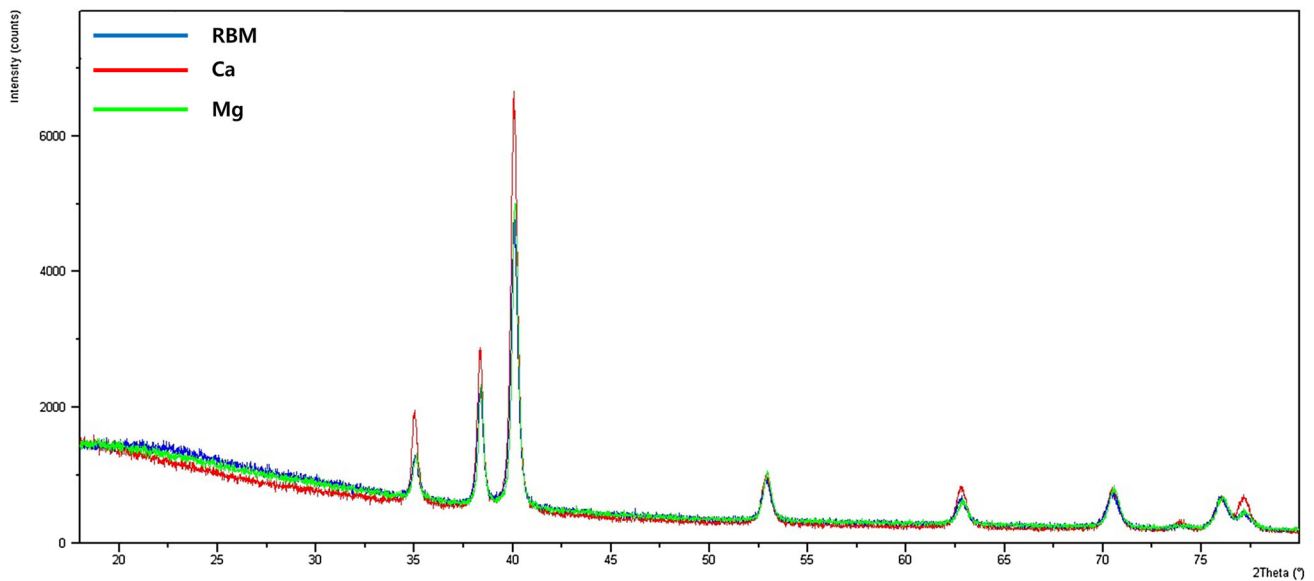
Fig. 2 X-ray diffraction pattern of the resorbable blast media (RBM) surface (*blue line*), the Ca ion-implanted surface (*red line*), and the Mg ion-implanted surface (*green line*). (Color figure online)
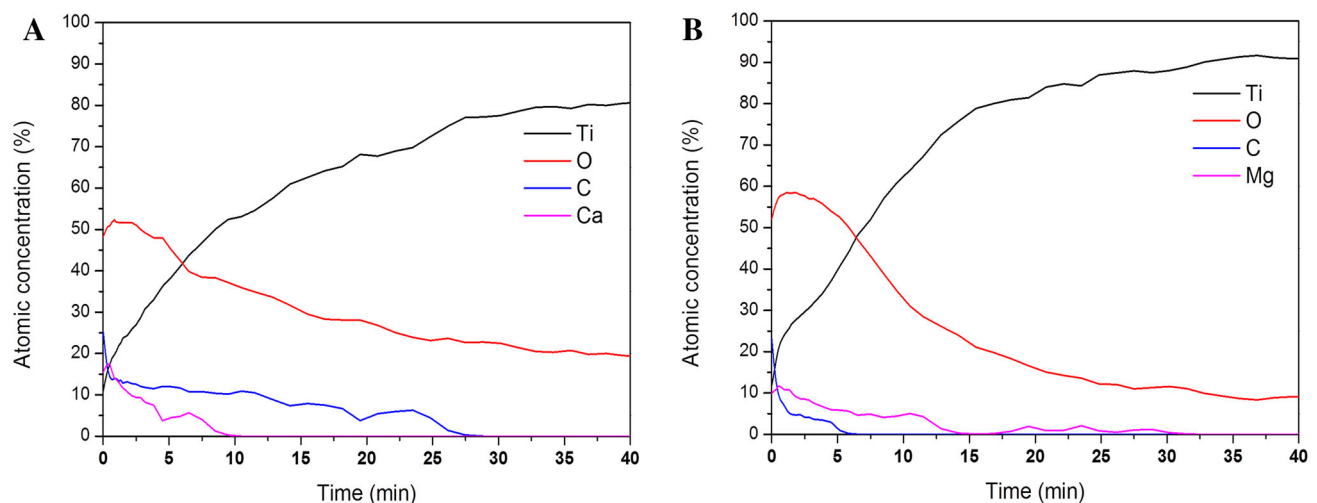

Fig. 3 Auger electron spectroscopy depth profiles of the Ca ion-implanted surface (**A**) and the Mg ion-implanted surface (**B**)

OC after 6 days of cultivation are shown in Fig. 6. The expression of RUNX2, a key transcriptional modulator of osteoblast differentiation, was higher in the Mg ion-implanted surface. There was higher expression of type I collagen on the Mg ion-implanted surface. The RBM surface showed higher expression of ALP, which is an early marker of osteogenic differentiation, and implicates the formation of HA crystals. However, expression of OC, a late marker of osteogenic differentiation and a major non-collagenic protein of the bone matrix, was lower in the Ca ion-implanted surface compared with the RBM and Mg ion-implanted surfaces.

4 Discussion

We evaluated the surface characteristics of, and the cellular response to, titanium surfaces that had been implanted with Ca and Mg ions using the PIIID technique. Two different ions (Ca and Mg) were used to investigate the effect of ion implantation. An RBM grit-blasted titanium surface, which is clinically acceptable and widely used in commercial dental implants, was used as a control group to compare clinical efficiency.

The results of this study demonstrated that initial cell attachment on a titanium surface can be improved by Ca
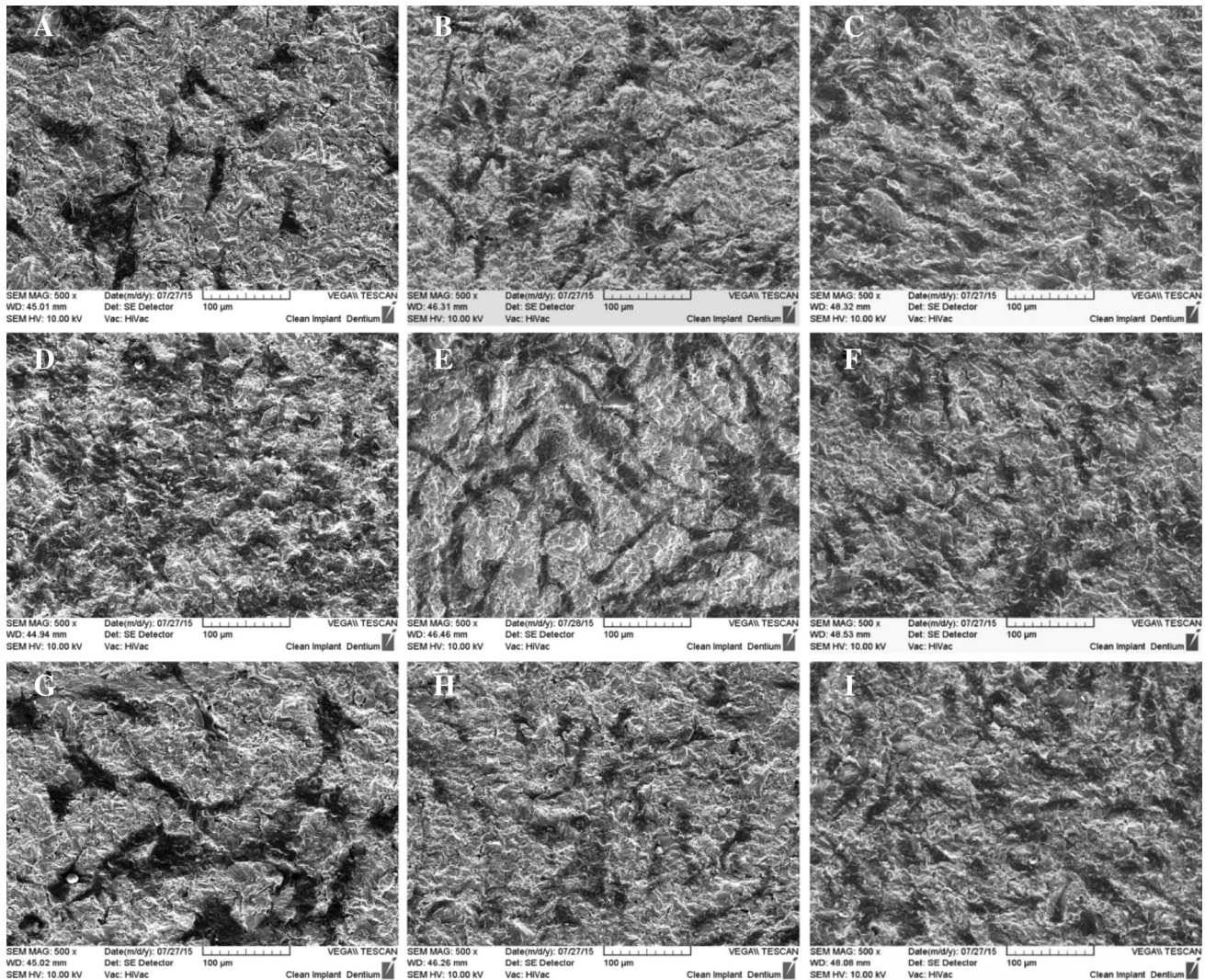
Fig. 4 Scanning electron microscope images of the resorbable blast media (RBM) surface (**A–C**), the Ca ion-implanted surface (**D–F**), and the Mg ion-implanted surface (**G–I**) at a magnification of ×500, after 4 h (**A, D, G**), 24 h (**B, E, H**), and 48 h of cultivation (**C, F, I**)
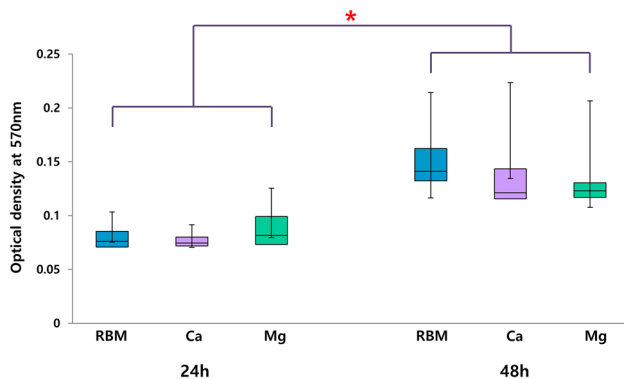

Fig. 5 Cell proliferation determined by 3-(4,5-dimethylthiazol-2-yl)-2,5-diphenyltetrazolium bromide (MTT) assay and expressed in terms of relative optical density at 570 nm

and Mg ion implantation. The SEM images of cells cultured on the Ca ion- and Mg ion-implanted surfaces exhibited a greater number of attached cells and improved quality of cell attachment with extended filopodia after 4 and 24 h of cultivation. These results agreed with those recently reported by researchers who investigated the advantages of chemically modified surfaces [30–32]. In these studies, ion-implanted surfaces showed a greater number of cells and improved quality of cell attachment, with flattened, elongated, stellate-shaped filopodia and developed lamellipodia extensions. However, in this study, all surfaces after 48 h of cultivation presented similar cellular attachment. This may have been due to the relative weakness of the initial effect of Ca and Mg chemistry on the successive cellular response.
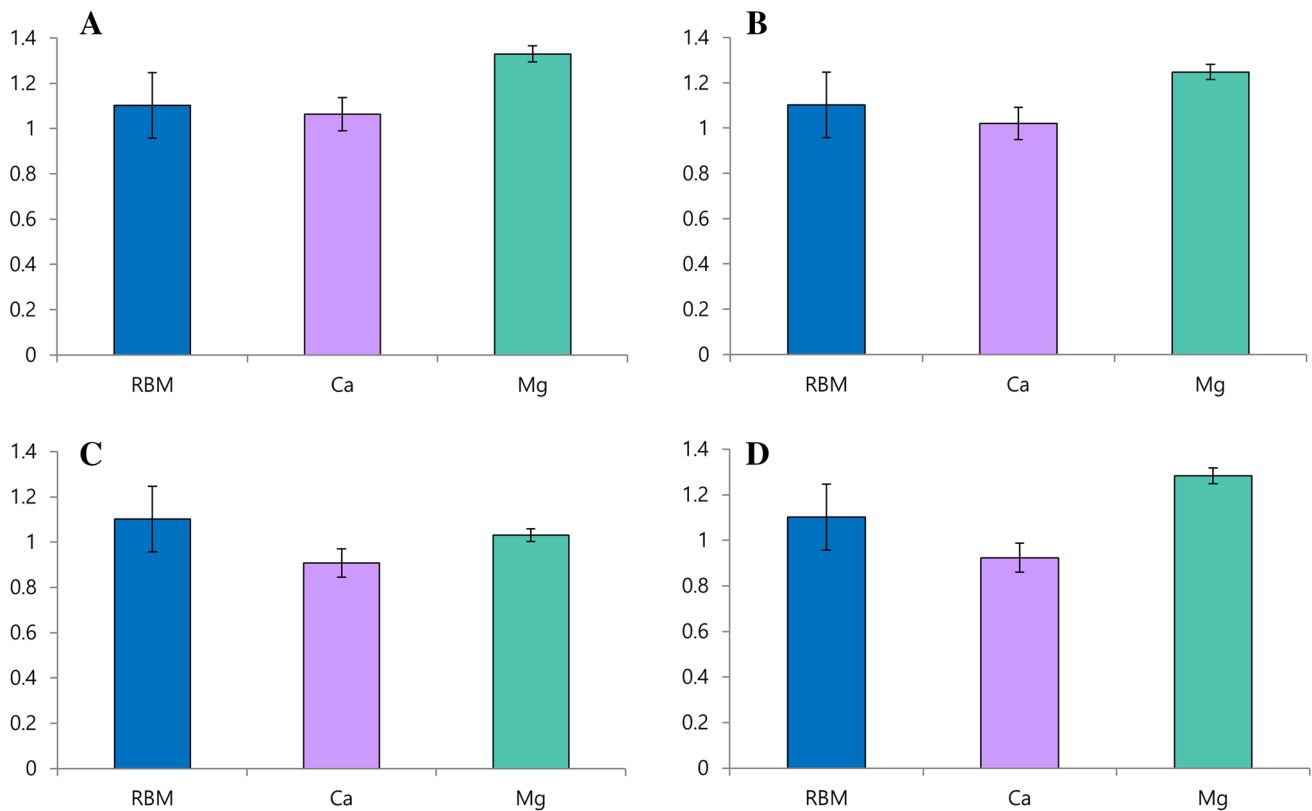
Fig. 6 Quantitative real-time polymerase chain reaction (PCR) analysis of the mRNA levels of **A** RUNX2, **B** type I collagen, **C** alkaline phosphatase (ALP), and **D** osteocalcin (OC) in hBM-MSCs on the three different surfaces after 6 days of cultivation

RBM grit-blasted titanium surfaces were used as a control group. Grit blasting is one of the approaches for roughening the titanium surface with ceramic particles. The blasting material should be chemically stable and biocompatible for osseointegration. However, the blasting particles often remain on the titanium surface and the residue is hard to remove, even after ultrasonic cleaning, acid passivation, and sterilization [33]. In this study, the RBM surface was grit-blasted with HA. Calcium phosphates, such as HA and β-tricalcium phosphate, can be used as biocompatible, osteoconductive, and resorbable blasting particles. Therefore, RBM surface treatment by grit blasting causes fewer concerns about residual particles comprising Ca and P, and can avoid impediments to osseointegration between the surrounding tissue and the titanium implant surface.

In this study, surface characteristics were evaluated by surface roughness (Ra) measurement, SEM, XRD, and AES depth profile investigation. The Ra values (0.91 to 0.92 μm) of the 3 different surfaces were categorized as minimally rough (ranging from 0.5 to 1.0 μm) and close to moderately rough (ranging from 1.0 to 2.0 μm), which are acceptable values for clinical dental implants that show good clinical results [34, 35]. SEM analysis revealed that the surfaces were similarly irregular and had a rough morphology, as was generally observed in grit-blasted surfaces. The surface roughness measurements and SEM analysis revealed that there was no topographical change after ion implantation by PIIID. The XRD analysis presented no newly formed compounds or changes to the crystalline structure after ion implantation by PIIID. AES analysis revealed that on the outermost surface, the atomic concentration of Ca ions was slightly greater than that of Mg ions; however, the atomic concentration of Mg ions was greater in the deeper layer. Total atomic concentrations of Ca and Mg ions in the implanted layer were similar according to calculations of the area under the concentration graph curve. Oxygen in the form of magnesium or calcium oxide may be considered to be derived from residual gas present during the ion implantation procedure [18]. More oxygen was found in the Ca ion-implanted layer owing to the high affinity of Ca ions for oxygen [21]. Carbon was considered to be a hydrocarbon contamination produced by ion implantation or sterilization [36, 37]. The greater quantities of carbon remnants at greater depths in the Ca ion-implanted surface may be one reason for the relatively low expression levels of type I collagen, ALP, and OC compared with the other surfaces. To sum up the surface analysis results, the ion implantation procedure using the PIIID technique resulted in a change in the

surface chemistry, such as the ion composition, but no change in the topography.

hBM-MSCs were used to determine cellular response to chemically modified titanium surfaces in this study. Mesenchymal stem cells and osteoprogenitor cells act as initial colonizers on titanium surfaces because they have the ability to migrate on osteoconductive surfaces. Thalji and Cooper [38] suggested that surface topography generally affects the pattern of gene expression for bone-related proteins (osteopontin, osteonectin, bone sialoprotein, type I collagen, and ALP). Moreover, RUNX2, a key factors in osteoinduction and transcription, affects osteoblast differentiation by controlling the osteoblast-specific gene expression (associated with osteogenesis) of type I collagen, ALP, osteopontin, and OC. In this study, RUNX2 presented higher expression on the Mg ion-implanted surface than on the other surfaces. This may be due to the synergistic effect of Mg ions resulting from PIIID and the Ca ions resulting from HA grit blasting as a pretreatment. However, the expression levels of type I collagen, ALP, and OC were relatively lower on the Ca ion-implanted surface than on the other surfaces. As mentioned above, this may be affected by an increased carbon remnant on the Ca ion-implanted surface.

Ion implantation changed the surface chemistry of the titanium and improved its biocompatibility and osteoconductivity without changing its topography. Ca and Mg ion are known to have an effect on the expression of genes related to bone formation and the binding interaction of cellular receptors [6, 23]. Therefore, in this study, the quality and quantity of initial cell attachment was superior in the Ca ion- and Mg ion-implanted surfaces than in the RBM-treated surface.

Although the Ca ion-implanted surface demonstrated great initial attachment, the expression of osteoblastic phenotypes related to osteogenesis (type I collagen, ALP, and OC) were relatively low compared with the other surfaces. Little is known about the osteoblastic differentiation of mesenchymal stem cells and carbon remnant contamination produced during the manufacturing process. In addition, the results of this study could be interpreted into that cell proliferation and differentiation are mainly affected by topographical characteristics. Surface chemistry modification by Ca ion and Mg ion implantation had an effect on cell attachment in the early stage, and a limited effect on cell proliferation and differentiation in the later stage.

Compliance with ethical standards

Conflicts of interest The authors have no financial conflicts of interest related to this study.

Ethical statement The authors have no ethical issues for human and animal right.

References

1. Schwartz Z, Boyan B. Underlying mechanisms at the bone–biomaterial interface. J Cell Biochem. 1994;56:340–7.
2. Wennerberg A, Albrektsson T. Effects of titanium surface topography on bone integration: a systematic review. Clin Oral Implants Res. 2009;20:172–84.
3. Manso M, Langlet M, Martınez-Duart J. Testing sol–gel $CaTiO_3$ coatings for biocompatible applications. Mater Sci Eng C Mater Biol Appl. 2003;23:447–50.
4. Kim H, Miyaji F, Kokubo T, Nakamura T. Preparation of bioactive Ti and its alloys via simple chemical surface treatment. J Biomed Mater Res. 1996;32:409–17.
5. Sul Y, Johansson CB, Röser K, Albrektsson T. Qualitative and quantitative observations of bone tissue reactions to anodised implants. Biomaterials. 2002;23:1809–17.
6. Hanawa T, Kamiura Y, Yamamoto S, et al. Early bone formation around calcium-ion-implanted titanium inserted into rat tibia. J Biomed Mater Res. 1997;36:131–6.
7. Sul Y, Byon EE, Jeong YY. Biomechanical measurements of Calcium-Incorporated oxidized implants in rabbit bone: effect of calcium surface chemistry of a novel implant. Clin Implant Dent Relat Res. 2004;6:101–10.
8. Mändl S, Krause D, Thorwarth G, et al. Plasma immersion ion implantation treatment of medical implants. Surf Coat Technol. 2001;142:1046–50.
9. Anders A. Handbook of plasma immersion ion implantation and deposition, vol. 8. New York: Wiley; 2000.
10. Byon E, Moon S, Cho S, Jeong C, Jeong Y, Sul Y. Electrochemical property and apatite formation of metal ion implanted titanium for medical implants. Surf Coat Technol. 2005;200:1018–21.
11. Ellingsen JE, Johansson CB, Wennerberg A, Holmen A. Improved retention and bone-to-implant contact with fluoride-modified titanium implants. Int J Oral Maxillofac Implants. 2004;19:659–66.
12. Sul Y, Johansson CB, Kang Y, Jeon D, Albrektsson T. Bone reactions to oxidized titanium implants with electrochemical anion sulphuric acid and phosphoric acid incorporation. Clin Implant Dent Relat Res. 2002;4:78–87.
13. Park J, Suh J, Chung H. Effects of calcium ion incorporation on osteoblast gene expression in MC3T3-E1 cells cultured on microstructured titanium surfaces. J Biomed Mater Res A. 2008;86:117–26.
14. Nayab S, Jones F, Olsen I. Human alveolar bone cell adhesion and growth on ion-implanted titanium. J Biomed Mater Res A. 2004;69:651–7.
15. Nayab SN, Jones FH, Olsen I. Effects of calcium ion implantation on human bone cell interaction with titanium. Biomaterials. 2005;26:4717–27.
16. Sul Y, Johansson P, Chang B, Byon E, Jeong Y. Bone tissue responses to mg-incorporated oxidized implants and machine-turned implants in the rabbit femur. J Appl Biomater Biomech. 2005;3:18–28.
17. Sul YT, Johansson C, Albrektsson T. Which surface properties enhance bone response to implants? Comparison of oxidized magnesium, TiUnite, and osseotite implant surfaces. Int J Prosthodont. 2006;19:319–28.
18. Cho L, Kim D, Kim J, Byon E, Jeong Y, Park C. Bone response of mg ion-implanted clinical implants with the plasma source ion implantation method. Clin Oral Implants Res. 2010;21:848–56.

19. Park J, Kim Y, Jang J, Song H. Osteoblast response to magnesium ion-incorporated nanoporous titanium oxide surfaces. Clin Oral Implants Res. 2010;21:1278–87.

20. Song W, Heo J, Lee J, Park Y, Kim Y. Osseointegration of magnesium-incorporated sand-blasted acid-etched implant in the dog mandible: resonance frequency measurements and histomorphometric analysis. Tissue Eng Regen Med. 2016;13:191–9.

21. Hanawa T, Ukai H, Murakami K. X-ray photoelectron spectroscopy of calcium-ion-implanted titanium. J Electron Spectrosc Relat Phenom. 1993;63:347–54.

22. Parise LV, Phillips DR. Fibronectin-binding properties of the purified platelet glycoprotein IIb–IIIa complex. J Biol Chem. 1986;261:14011–7.

23. Mould AP, Akiyama SK, Humphries MJ. Regulation of integrin α5β1-fibronectin interactions by divalent cations evidence for distinct classes of binding sites for Mn^{2+}, Mg^{2+}, and Ca^{2+}. J Biol Chem. 1995;270:26270–7.

24. Krause A, Cowles EA, Gronowicz G. Integrin-mediated signaling in osteoblasts on titanium implant materials. J Biomed Mater Res. 2000;52:738–47.

25. Zreiqat H, Howlett C, Zannettino A, et al. Mechanisms of magnesium-stimulated adhesion of osteoblastic cells to commonly used orthopaedic implants. J Biomed Mater Res. 2002;62:175–84.

26. Cooper LF, Masuda T, Whitson SW, Yliheikkila P, Felton DA. Formation of mineralizing osteoblast cultures on machined, titanium oxide grit-blasted, and plasma-sprayed titanium surfaces. Int J Oral Maxillofac Implants. 1999;14:37–47.

27. Caplan AI. Mesenchymal stem cells. J Orthop Res. 1991;9:641–50.

28. Wang C, Zhao B, Ai H, Wang Y. Comparison of biological characteristics of mesenchymal stem cells grown on two different titanium implant surfaces. Biomed Mater. 2008;3:015004.

29. Kassem M. Mesenchymal stem cells: biological characteristics and potential clinical applications. Cloning Stem Cells. 2004;6:369–74.

30. Cecchinato F, Xue Y, Karlsson J, et al. In vitro evaluation of human fetal osteoblast response to magnesium loaded mesoporous TiO_2 coating. J Biomed Mater Res A. 2014;102:3862–71.

31. Kim B, Kim JS, Park YM, Choi B, Lee J. Mg ion implantation on SLA-treated titanium surface and its effects on the behavior of mesenchymal stem cell. Mater Sci Eng C. 2013;33:1554–60.

32. Cheng M, Qiao Y, Wang Q, et al. Calcium plasma implanted titanium surface with hierarchical microstructure for improving the bone formation. ACS Appl Mater Interfaces. 2015;7:13053–61.

33. Le Guéhennec L, Soueidan A, Layrolle P, Amouriq Y. Surface treatments of titanium dental implants for rapid osseointegration. Dent Mater. 2007;23:844–54.

34. Albrektsson T, Wennerberg A. Oral implant surfaces: part 1—review focusing on topographic and chemical properties of different surfaces and in vivo responses to them. Int J Prosthodont. 2004;17:536–43.

35. Albrektsson T, Wennerberg A. The impact of oral implants-past and future, 1966–2042. J Can Dent Assoc. 2005;71:327.

36. Lausmaa J. Surface spectroscopic characterization of titanium implant materials. J Electron Spectrosc Related Phenom. 1996;81:343–61.

37. Gittens RA, Olivares-Navarrete R, Cheng A, et al. The roles of titanium surface micro/nanotopography and wettability on the differential response of human osteoblast lineage cells. Acta Biomater. 2013;9:6268–77.

38. Thalji G, Cooper LF. Molecular assessment of osseointegration in vivo: a review of the current literature. Int J Oral Maxillofac Implants. 2013;28:e521–34.